# Exposure to Non-exhaust Emission in Central Seoul using an Agent-based Framework

Hyesop Shin[1][0000−0003−2637−7933] and Mike Bithell[2]

[1] School of Geographical and Earth Sciences, University of Glasgow, G12 8QQ, UK
[2] Deptartment of Geography, University of Cambridge, CB2 3EN, UK
Hyesop.Shin@glasgow.ac.uk

**Abstract.** Non-exhaust emission (NEE) from brake and tyre wear cause deleterious effects on human health, but relationship with mobility has not been thoroughly examined. We construct an *in silico* agent-based traffic simulator for Central Seoul to illustrate the coupled problems of emissions, behaviour, and the estimated exposure to $PM_{10}$ (particles less than 10 microns in size) for groups of drivers and subway commuters. The results show that significant extra particulates relative to the background exist along roadways where NEEs contributed some 40% of the roadside $PM_{10}$. In terms of health risk, 88% of resident drivers had an acute health effect in late March but that kind of emergence rarely happened. By contrast, subway commuters' health risk peaked at a maximum of 30% with frequent oscillations whenever the air pollution episodes occurred. A 90% vehicle restriction scenario reduced $PM_{10}$ by 18-24%, and reduced the resident driver's risk by a factor of 2, but not effective for subway commuters as the group generally walked through background areas rather than along major roadways. Using an agent-based traffic simulator in a health context can give insights into how exposure and health outcomes can depend on the time of exposure and the mode of transport.

**Keywords:** Agent-based Traffic Simulation · Non-Exhaust Emission · Exposure and Health Loss · NetLogo

## 1 Introduction

Traffic-related air pollution (TRAP) has long been associated with adverse health outcomes. The book *Non-exhaust emissions (NEE): an urban air quality problem for public health* compiled recent scientific findings that addressed non-exhaust particles which are formed of metallic, rubber, carbon black, and other organic substances by combustion, wear, road abrasion, and particle resuspension [2]. All of these substances are as equally catastrophic as exhaust particles.

NEE can be affected by traffic queues, driving behaviour, and weather. In traffic congestion, the 'stop-and-go' patterns of the traffic generate more wear on brake pads and discs that adds to surges of ambient particulates during rush hours [1,4]. Brake wear emissions are also spatially heterogeneous because the vehicles would be expected to slow down when reaching a junction or going downhill [1,16]. In addition, harsh braking and acceleration can generate more

particles from tyres, brake discs, and linings. Transport for London has mentioned that the Central Business District (CBD) of London is more polluted than the outer areas, regardless of 20mph speed limits [17]. The expert group pointed out a strong relationship between aggressive driving behaviour and more dispersion of particulate emission to the sidewalks that can possibly cause adverse health consequence. Although the regulation for NEE has not yet been made, the UK's Air Quality Expert Group (2019) [1] and the European Environmental Agency (2019) [6] have both reported the severity of NEE to human health and are calling for more evidence.

To this end, the European Environmental Agency (EEA) is the only institute that estimated a traffic-based NEE based on their research [6]. According to the research, NEE is calculated by four components, road wear, brake wear, surface wear, and resuspension. The emission levels vary by the number of vehicles within the unit distance (g/km), their mileage, emission factor, and speed characteristics. While the information is advantageous to understand the annual outcomes as a city-scale, the deterministic model limits the spatial dynamics of air pollution driven by traffic flows on a finer time scale.

To link the challenges between NEE and the mobility of vehicles and humans, agent-based modelling (ABM) is one of the key methods that can simulate urban traffic and air quality on an individual level [18]. ABM not only can simulate the movement of heterogeneous vehicles and individuals but also measures the exposure level based on the path on which the agent is situated and the estimated local pollution value [5,8,20]. A promising example is [8]'s integrated model, where it integrated $NO_x$ emission, dispersion, activity patterns of population, vehicle movement, and the exposure to the ambient $NO_x$ based on the time spent in each locations - has not been attempted previously. Other agent-based traffic models also have simulated vehicle emissions caused by urban car traffic using general programming language [9], SUMO [3,11], or MATSim [10].

This paper examines the exposure and possible health effects of NEE on commuter's health based on a traffic simulation. The specific questions are as follows:

- What is the difference in health effects between walking commuters and vehicle commuters?
- How did air quality improve as a result of the simulation of policy scenarios, and what were the characteristics of any improvements?

Given the limited resources available to mimic the agents' attributes and their behavioural patterns, we built an *in silico* agent-based traffic model.

## 2 Methods

### 2.1 Overview

Fig.1 illustrates the overall procedure of this study. This study retrieved hourly pollution, Seoul population, origin-destination by sub-district level, and traffic observation from the census and Seoul Institute. The remainder of this section describes a summarised ODD protocol, sensitivity analysis, and calibration.

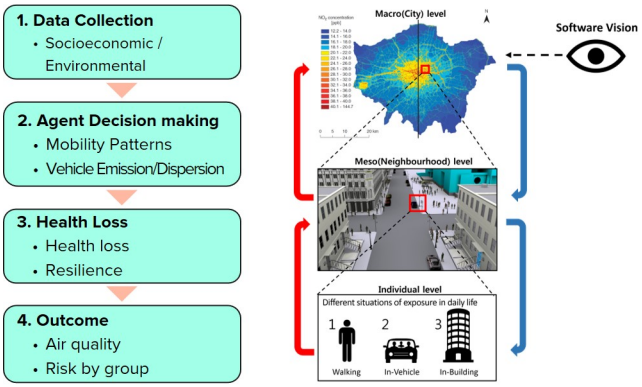


**Fig. 1.** A flowchart of the methodological procedure of the model (left), the agent types, and the vision of software (right)

### 2.2 A Summarised ODD Protocol

A complete, detailed model description, following the ODD (Overview, Design concepts, Details) protocol [7] is provided in the supplementary material [15]. The purpose of this model is to understand commuter's exposure to non-exhaust $PM_{10}$ emissions, and to make a preliminary estimate of their health effects. We use the following patterns of the 'at-risk' population by transport modes, traffic volume by road, and pollution levels by road in a context that is representative of realistic conditions in the Seoul CBD.

The model includes the following entities of three mobile agents: (1) resident cars with drivers, (2) non-resident cars[3], and (3) subway commuters; and two fixed agents: (1) traffic signals, and (2) entry points where the vehicles are fed into the study area. The state variables and attributes characterising these entities are listed in the repository [15]. The spatial and temporal resolution of the study area, is 30m×30m and 1 minute respectively. Our study area is the CBD of Seoul (16.7km$^2$), which in in the NetLogo model consists of 155 horizontal and 192 vertical patches. The model is implemented for 3 months between January and March 2018 (approx. 130,000 ticks).

The most important processes of the model, which are repeated every time step, are the update of particulates on roads and background areas, the journey of vehicles and pedestrians, and the exposure and health loss in response to mobility patterns and non-exhaust $PM_{10}$ emissions. The agents are assumed to have a healthy medical profile at the beginning of the simulation, but are expected to have their health decreased when they are exposed to over 100µg/m$^3$ of $PM_{10}$. Subway commuting agents are assumed to be exposed to the ambient level $PM_{10}$ between early morning and late in the evening even if they do not appear on

[3] We clarify that non-resident vehicles are those for which the origin is outside the model domain. For example delivery vehicles - routing these non-randomly would require knowing both intermediate and final destination data. For the present, we treat these as random as this is better than omitting them completely, but the model might be improved with knowledge of where they were headed

the interface. If the health of an agent drops to a third of the initial state, the model will recognise the individual to be 'at-risk'. The cumulative updates of the 'at-risk' population and the $PM_{10}$ concentration by roads are exported to a spreadsheet at the end of the simulation.

The most important concept of the model is emergence and stochasticity. The emergence of the 'at-risk' population (i.e. those with health under a third of the initial health status) occurs from a balance between exposure to a $PM_{10}$ threshold of 100µg/$m^3$ and recovery. The threshold is referred to the hourly standard controlled by the S.Korean government. Stochasticity is another crucial component because (1) the number of non-resident vehicles within the study area can cause traffic congestions at any junction given that the vehicles move randomly, and (2) the infiltration ratio (indoor-to-outdoor concentration ratio) varies by the microenvironment and the time spent. This study estimates the infiltration from the ambient $PM_{10}$ of the current patch to indoor spaces such as houses between 0.2-0.7 [12,13], workplaces at 0.2 [12], and transits - i.e. subway and in-vehicles at 0.7 [12].

The model is initialised with a 1% sample of 69,806 resident vehicles with unleaded, diesel, and LPG fuel tanks, and 1% sample of 193,200 subway commuters. The resident drivers who commuted beyond our study area were removed, which resulted in 399 driving agents and 1,932 subway agents. During weekdays, trips are made along the shortest path and will not change throughout the simulation, except weekends where the agents have freedom to choose their trips and return before the weekday starts. Since the aggregated OD information cannot provide the exact location of agents, we allow some randomness to allocate the origin and destinations for each simulation run.

Key processes in the model are the pathfinding algorithms, and the generation and dispersion of NEEs. For vehicle pathfinding (see Fig.2), we initially retrieved road networks and removed minor streets, then employed an A* algorithm for each vehicle to find the shortest path while avoiding dead ends and obstacles [21]. As explained above, LSA is used for pedestrians to navigate the shortest distance from origin to goal, which in this case is a straight line. This algorithm may allow many agents to penetrate buildings during their journey, which is somewhat awkward. The LSA algorithm was compared with a different set of code that asked the agents to bypass buildings. However, the alternative code set took much longer execution time while the exposure levels hardly showed any difference.

To generate NEE from each vehicle, we transform the EEA's trip-based NEE equation (g/km) to a unit-based emission (patch-by-patch) in order to mimic the distribution of emission sources [6]. We use `µg/30m` to match the spatial resolution (patch) of the model environment.

## 3 Sensitivity Analysis

This study uses one-factor-at-a-time (OFAT) method to examine the sensitivity for each of the parameters. Since computational limitations are made more, it

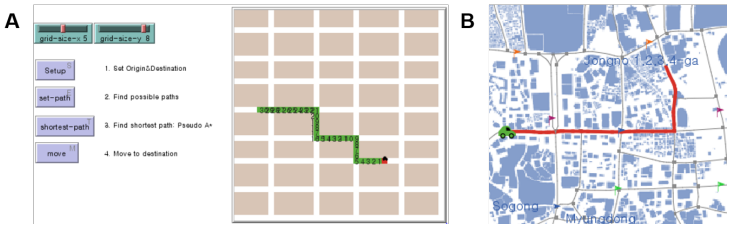


**Fig. 2.** (A) is a test of an agent finding the shortest path from the origin (red patch) to its destination (light green patch) based on A*, and (B) is the application of A* for a sample vehicle used in study site

is normal that full-factorial parameterisation should be considered. However, we did not find any noticeable interaction effects in the outcome after testing the combinations between emission, dispersion, and dilution over a selected period. Each parameter is analysed from an average of 20 iterations to reduce possible stochastic effects.

### 3.1 Dispersion and Dilution

We parameterise the angle of dispersion from each vehicle to understand whether wider impact of non-exhaust $PM_{10}$ to the neighbouring patches affects more risk to people; and the adjust the 'time until this dispersion dilutes' (see Fig.3). The baseline parameters enable vehicles to disperse 1) in a cone behind the vehicle with an angle of 60° and 2) dilute within 0-3 minutes at which the particles effectively settles out. 60° approximately accounts for 5-7 patches of $PM_{10}$.

By controlling the dilution parameter by $< 3$ ticks (i.e. allowing the model to give an integer between 0 and three at random), the first experiment simulates the range of dispersion at 45° and 90°. Then, controlling the dispersion to 60°, we increase the time of dilution by $5+\beta$ ticks ($0<\beta<5$) and $10+\theta$ ticks ($0<\theta<10$).

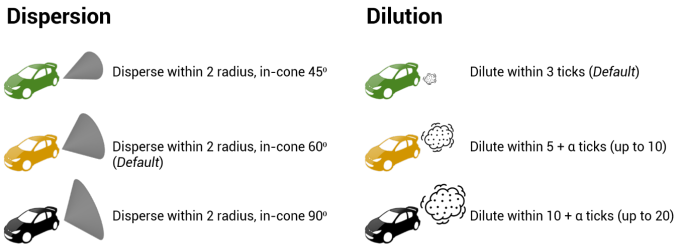


**Fig. 3.** Illustrations of dispersion parameters (left) and dilution parameters (right)

Results show that dispersion angle of each vehicle did not change the roadside $PM_{10}$ in most of the stations, except for Jongno, where the difference varied by an average of 3µg/m$^3$ at `Emission 5` and 14µg/m$^3$ at `Emission 20` (see Table 1). Looking at the station's location in the real world as well as the model, Jongno

was the only curbside station that was under 3 metres from the main road while the others were much indented to the pavements. If the monitors in other roads were close enough to the road, the outcomes could have been similar to Jongno.

**Table 1.** $PM_{10}$ concentrations by emission factors and dispersion range ($\mu g/m^3$)

| Emission | Cone Width (°) | Jongno | Sejong | Yulgok | Samil | Pirun |
|---|---|---|---|---|---|---|
| 5 | 45 | 58.4 | 55.7 | 58.7 | 58.9 | 60.1 |
| | 60 | 59.3 | 56.3 | 59 | 59.5 | 60.4 |
| | 90 | 60.4 | 56.6 | 59.1 | 59.5 | 60.8 |
| 10 | 45 | 73.2 | 71.2 | 77.3 | 77 | 80.5 |
| | 60 | 76.6 | 72.3 | 77.9 | 77.4 | 81 |
| | 90 | 79.6 | 73.1 | 78.5 | 78.1 | 81.8 |
| 20 | 45 | 102 | 100 | 112 | 113 | 118 |
| | 60 | 109 | 102 | 114 | 115 | 120 |
| | 90 | 116 | 104 | 115 | 118 | 120 |

Unlike the dispersion results, all roads were very sensitive to the dilution period (see Table 2). In `Emission 5`, the default period of less than 3 minutes indicated an average figure of 60-62$\mu g/m^3$, however, extending the period to 10 minutes increased $PM_{10}$ to 67-69$\mu g/m^3$, which was 10% higher than the default.

The difference between dilution periods increased proportionately to emission factors, where the quickest dilution (0-3 mins) turned out to be 14-18$\mu g/m^3$ lower on average than the slower dilution (particles maintaining in the patch) when we tested `Emission 10`, and 31-41$\mu g/m^3$ lower when `Emission 20` was tested. If this analysis was to represent the length of dust emission and resuspension in the real world, say 3 minutes of dust floating until dilution, the decrease of $PM_{10}$ can be explained by the floating particles from the vehicles mixing well with the atmosphere. A disclaimer is that the dilution is only affected by the duration of ticks (zero wind), and no other components (e.g. wind, rain) that change dilution time. Note we tested `Emission 1` but did not find a significant difference to any parameters.

### 3.2 Health Loss & Recovery

*Context* The percentage of the population at risk (i.e. those with health under 100) emerges from a balance between exposure to a $PM_{10}$ threshold of 100$\mu g/m^3$ and recovery. In practice, the emergence can be an acute response to $PM_{10}$ exposure before the natural recovery begins to take effect. The emergence pattern will differ by which means of transport the individual is commuting with. The agent's health will decline on the assumption that it encounters over 100$\mu g/m^3$ where they are currently located.

$$IfPM_{10} \geq 100, \qquad \frac{dH}{dT} = -\alpha(H_{\max} - H(t)) + H_{\text{recov}} \tag{1}$$

In Equation (1), $H_{max}$ denotes an agent's health status at the beginning and H(t) is strictly less than $H_{max}$. H(t) is the current value, and $H_{recov}$ is the recovery

**Table 2.** $PM_{10}$ concentrations by emission factors and (the duration until) dilution ($\mu g/m^3$)

| Emission | Duration | Jongno | Sejong | Yulgok | Samil | Pirun |
|---|---|---|---|---|---|---|
| | 3 | 45.5 | 45.8 | 45.8 | 46 | 46.1 |
| 1 | 5 | 46.1 | 46 | 46.5 | 46.2 | 46.4 |
| | 10 | 46.7 | 46.5 | 46.8 | 46.7 | 47 |
| | 3 | 60 | 60 | 62 | 62 | 62 |
| 5 | 5 | 66 | 66 | 66 | 66 | 67 |
| | 10 | 67 | 67 | 68 | 68 | 69 |
| | 3 | 81 | 81 | 86 | 85 | 85 |
| 10 | 5 | 94 | 95 | 96 | 96 | 99 |
| | 10 | 99 | 99 | 100 | 100 | 102 |
| | 3 | 123 | 123 | 134 | 133 | 133 |
| 20 | 5 | 153 | 150 | 155 | 155 | 159 |
| | 10 | 164 | 160 | 165 | 164 | 167 |

rate. If the agent is on the patch that exceeds the $PM_{10}$ threshold of 100, its health values would decrease exponentially away from their initial value H(0). The factor $\alpha$ sets the rate of change per unit of time when the health impact applies. This factor is chosen from a random uniform distribution between zero and a maximum on each tick to allow for the fact that, even within a patch, since these are 30m across, the individual exposure levels will be very different.

*Output* To test the sensitivity of health loss parameters, we adjust the $\alpha$ from Equation 1 at `0.1`, `0.15`, and `0.2`.

For subway commuters, the at-risk emergence is discovered on January 20th-22nd, late February, and early&late March (see Fig.4). The maximum risk rate was 30% in `0.1`, but skyrocketed to 100% over `0.15`. Although a lot of uncertainty from other parameters has contributed towards the outcomes, the tipping point of the health loss parameter is somewhere between `0.1` and `0.15`. Several oscillations were also discovered during the extreme $PM_{10}$ events. This was because subway commuters have different commute hours that led them to be exposed to ambient $PM_{10}$.

Resident drivers experience fewer occurrences of health risk between `0.05` and `0.15`, which can be compared on the dates of January 22nd, February 12th, and March 8th. On March 24-25th, however, the majority of drivers suddenly experienced health risk due to the continuation of extreme $PM_{10}$ occurred during March 24-25th. While resident drivers had a relatively short period of commute time that prevented frequent health risk, the extreme levels of $PM_{10}$ led most of the drivers to an acute health crisis.

### 3.3 Walking Speed

We adjust various levels of walking speed for subway commuters to test how walking speed affects the degree of risk population (see Table **??**). Given the default speed at 0.5-0.9, the section tested 1) 0.2-0.4 patch per minute, and 2) 0.4-0.7 patch per minute. The range is given under the assumption that people have

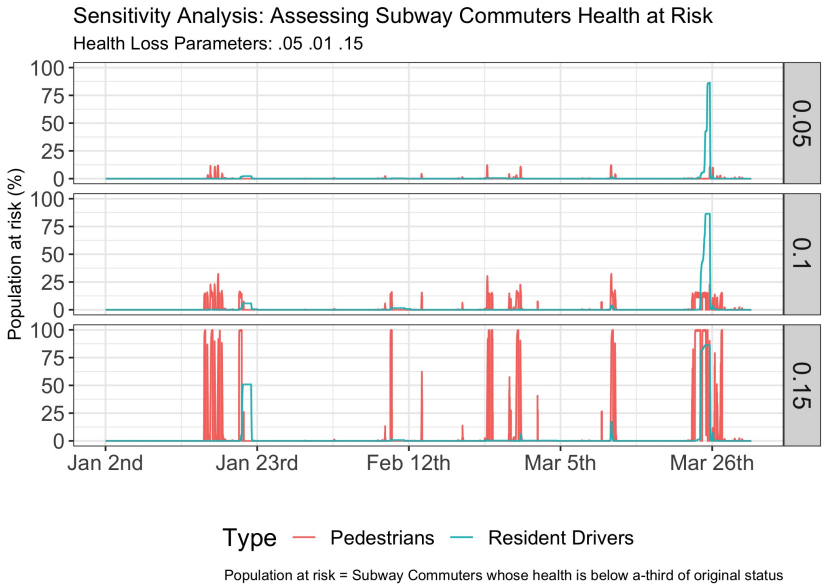


**Fig. 4.** Temporal change of risk rates for subway commuters (% of those with health under 100)

different walking speeds. Walking speed over 0.5 might seem rather unrealistic, but this experiment intends to illustrate how speed affects exposure levels.

The time series graph clearly show that the onset and peak levels are very sensitive to walking speed (see Fig.5). When the pedestrian's walking speed was 'Extremely Slow' (0.2-0.4), more than 40% of the population is at risk on five different occasions with the highest peak of 47%. However, the risk rate declines by 10% when the walking speed increased to 'Slow' (0.4-0.7) and further declines by 30% when the speed increased to 1.6-1.8. This corresponds to the previous sensitivity analyses because slowing down the walking speed can mean that the person is prolonging the exposure time, which in turn causes a further health loss.

## 4 Scenario Forecasting

Once the parameters are calibrated, we conduct 'what-if' scenarios to understand 1) how vehicle restrictions can improve air quality, and 2) the consequent health outcomes. As with the sensitivity section, the models were averaged from 20 iterations.

### 4.1 Vehicle Restriction

In Fig.6, traffic levels cut by 50% can result in a reduction of 1.2-2.7$\mu g/m^3$ (2-4%) of $PM_{10}$, while a further restriction by 90% of the normal traffic significantly can

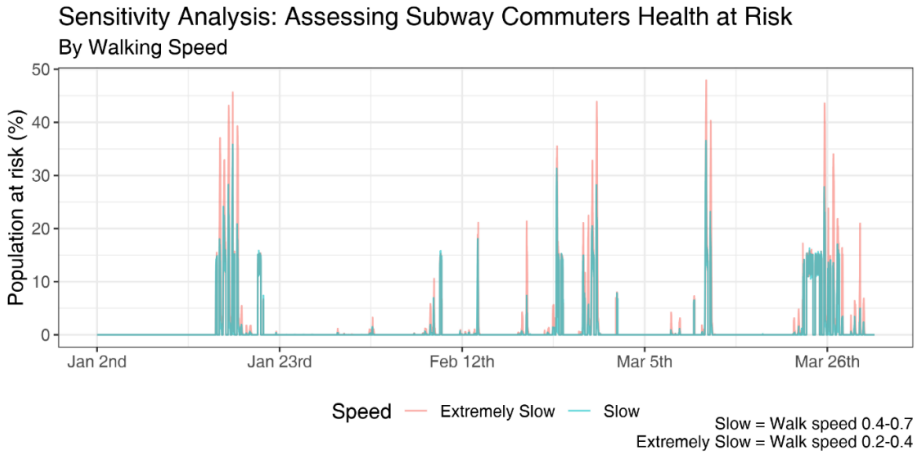


**Fig. 5.** Assessing subway commuters' health by different walking speed parameters

reduce $PM_{10}$ in the study area by 11.4-15.7µg/$m^3$ (18-24%) (see also Table 3). It is quite uncertain whether vehicle restriction scenarios without considering the meteorological effects would entail a realistic figure, but according to [14]'s work - 50% cut of brake disc emissions led to a 4-14% reduction in ambient $PM_{10}$ - we at least can suggest that Seoul's vehicle restriction plan can curb $PM_{10}$ by a significant level.

**Table 3.** Overall average of $PM_{10}$ on five roads by car restriction scenarios

| Scenario | Type | Jongno | Sejong | Yulgok | Samil | Pirun |
|---|---|---|---|---|---|---|
| Business as Usual | $PM_{10}$ | 60.7 | 61.3 | 62.5 | 62.4 | 63.6 |
| 50% Restriction | $PM_{10}$ | 58.0 | 59.6 | 60.2 | 61.2 | 61.3 |
| | Difference to BAU | 2.7 | 1.7 | 2.3 | 1.2 | 2.3 |
| 90% Restriction | $PM_{10}$ | 47.9 | 49.8 | 48.1 | 51.0 | 47.9 |
| | Difference to BAU | 12.8 | 11.5 | 14.4 | 11.4 | 15.7 |

### 4.2 Health Loss from NEE and $PM_{10}$ Exposure

Our subsequent scenario is whether the vehicle restriction lead to less harm to health. As a result, over 10% of drivers were put into risk on January 23rd 2018, but when the incoming vehicles were cut by 90%, the 'at risk' drivers reduced by 5% (see Fig.7A), which seemed to be effective. However, it could not prevent the surge of health risks at late March when roadside and background $PM_{10}$ were both persistently high (<1% difference).

In contrast, restricting vehicles did not seem to be effective on pedestrians (see Fig.7B). This was because most pedestrians walked on the background path-

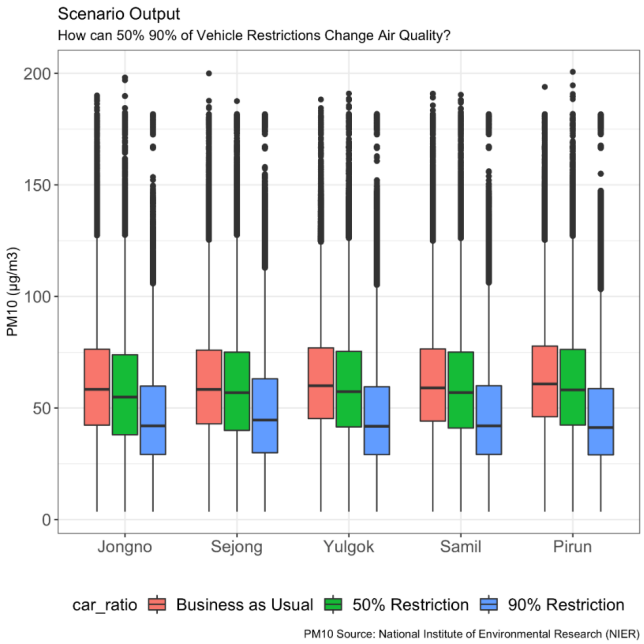


**Fig. 6.** Boxplot of $PM_{10}$ by each restriction scenario

ways and their long commute time escalated the chance to get exposed to high $PM_{10}$.

It is worth pointing out that the 'alarmingly high' days of ambient $PM_{10}$ as well as the sudden increase of roadside $PM_{10}$ happens more frequently in Seoul during the winter period. Even worse, the particulates tend to remain in the atmosphere as the 'bowl-shaped' topography of central Seoul resist the wind speed.

## 5 Conclusion

This paper investigated a traffic simulation for central Seoul to investigate the coupled problem of NEE and exposure to $PM_{10}$ in groups of pedestrians and resident drivers. In summary, road traffic was found to have contributed around 40% of the average roadside $PM_{10}$ concentrations, with much higher contributions on a finer time scale. The rise of $PM_{10}$ was largely due to the amount of traffic that emitted NEE on roads, regardless of the fuel type and mode of power [1]. These findings are consistent with the case study of [19], where 48% of roadside $PM_{10}$ in Ruhr was contributed by particulate emissions, but because the "48%" figure was a summation of emissions from both exhaust and non-exhaust $PM_{10}$, the non-exhaust $PM_{10}$ emission alone are closer to the findings of this study. In addition, longer exposure for pedestrians led to a larger accumulated exposure overall, the majority of drivers were exposed to the highest levels of

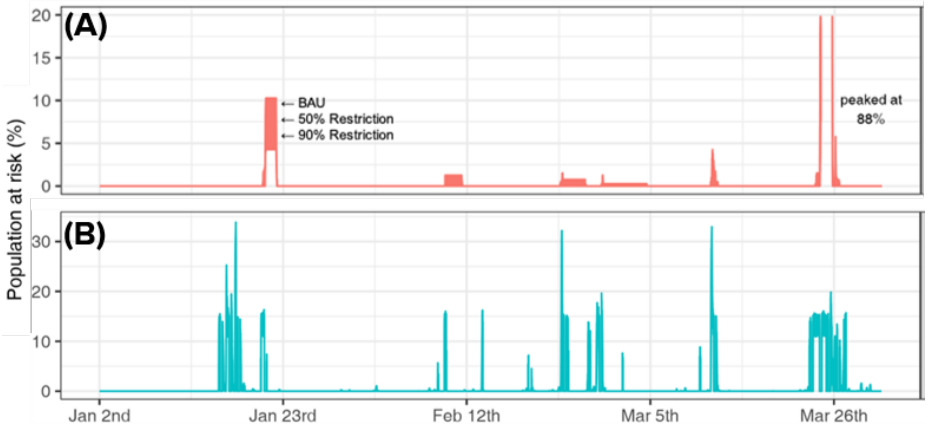


**Fig. 7.** Health risk of resident vehicle drivers (A) and subway commuters (B)

pollution (>150µg/m$^3$), which was largely due to the time spent in congested areas. The health effects, however, depended strongly on how the impact and recovery from exposure were parameterised.

In the vehicle restriction scenario, roadside $PM_{10}$ showed a 18-24% (11-17µg/m$^3$) decrease when the majority of cars (90%) were banned from the city centre, while an average of 2-5µg/m$^3$ decrease was seen in the study area when 50% ban was implemented. In other words, at least 90% of vehicle reduction is a noticeable level for air quality improvement. Upon our further investigation on vehicle restriction and health effects, we found a decent improvement of health risk to drivers happen when 90% ban scenario was introduced but unable to seek a similar effect on subway commuters.

This study was the first to jointly examine the contribution of NEEs and the adverse health effects on a group of commuters from a microscopic approach. The application of NEEs on a patch level sufficiently recreated the generation of brake and tyre wear and the following dispersion that can possibly happen in the real world. Perceiving the severity of NEE to ambient $PM_{10}$, future studies should consider more sophisticated ways that particles from brakes and tyre wear are generated and dispersed on roads, and whether the shortest-distance trip on major roads is better than taking a less congested route but one with extended travel time in terms of reducing one's exposure level.

## References


1. Air Quality Expert Group: Non-Exhaust Emissions from Road Traffic. Tech. rep., Department for Environment, Food and Rural Affairs (2019)
2. Amato, F.: Non-exhaust emissions: an urban air quality problem for public health; impact and mitigation measures. Academic Press (2018)
3. Anjum, S.S., Noor, R.M., Aghamohammadi, N., Ahmedy, I., Kiah, L.M., Hussin, N., Anisi, M.H., Qureshi, M.A.: Modeling traffic congestion based on air quality for greener environment: an empirical study. IEEE Access **7**, 57100–57119 (2019)
4. Cambridge Insight: Cambridge Transport and Health. Tech. rep., Cambridge Insight (2017), `https://cambridgeshireinsight.org.uk/environment/airquality/`
5. Crooks, A., Malleson, N., Manley, E., Heppenstall, A.: Agent-Based Modelling and Geographical Information Systems: A Practical Primer (Spatial Analytics and GIS). SAGE Publications Ltd, 1 edn. (2019)
6. EMEP/EEA: EMEP/EEA Air Pollutant Emission Inventory Guidebook 2019. Tech. rep., European Environment Agency (2019), `https://www.eea.europa.eu/publications/emep-eea-guidebook-2019/part-b-sectoral-guidance-chapters/1-energy/1-a-combustion/1-a-3-b-vi/view`
7. Grimm, V., Railsback, S.F., Vincenot, C.E., Berger, U., Gallagher, C., DeAngelis, D.L., Edmonds, B., Ge, J., Giske, J., Groeneveld, J., Johnston, A.S., Milles, A., Nabe-Nielsen, J., Polhill, J.G., Radchuk, V., Rohwäder, M.S., Stillman, R.A., Thiele, J.C., Ayllón, D.: The odd protocol for describing agent-based and other simulation models: A second update to improve clarity, replication, and structural realism. Journal of Artificial Societies and Social Simulation **23**(2), 7 (2020). https://doi.org/10.18564/jasss.4259, `http://jasss.soc.surrey.ac.uk/23/2/7.html`
8. Gurram, S., Stuart, A.L., Pinjari, A.R.: Agent-based modeling to estimate exposures to urban air pollution from transportation: Exposure disparities and impacts of high-resolution data. Computers, Environment and Urban Systems **75**(April 2018), 22–34 (2019). https://doi.org/10.1016/j.compenvurbsys.2019.01.002, `https://doi.org/10.1016/j.compenvurbsys.2019.01.002`
9. Hofer, C., Jäger, G., Füllsack, M.: Large scale simulation of co2 emissions caused by urban car traffic: An agent-based network approach. Journal of Cleaner Production **183**, 1–10 (2018). https://doi.org/https://doi.org/10.1016/j.jclepro.2018.02.113, `https://www.sciencedirect.com/science/article/pii/S0959652618304256`
10. Hülsmann, F., Gerike, R., Ketzel, M.: Modelling traffic and air pollution in an integrated approach - the case of Munich. Urban Climate **10**, 732–744 (2014). https://doi.org/10.1016/j.uclim.2014.01.001
11. Krajzewicz, D., Behrisch, M., Wagner, P., Luz, R., Krumnow, M.: Second generation of pollutant emission models for SUMO. In: Modeling mobility with open data, pp. 203–221. Springer (2015)
12. Kreider, M.L., Unice, K.M., Panko, J.M.: Human health risk assessment of Tire and Road Wear Particles (TRWP) in air. Human and Ecological Risk Assessment **0**(0), 1–19 (2019). https://doi.org/10.1080/10807039.2019.1674633, `https://doi.org/10.1080/10807039.2019.1674633`
13. Leung, D.Y.C.: Outdoor-indoor air pollution in urban environment: challenges and opportunity. Frontiers in Environmental Science **2**, 69 (2015). https://doi.org/10.3389/fenvs.2014.00069, `https://www.frontiersin.org/article/10.3389/fenvs.2014.00069`

14. Perricone, G., Matějka, V., Alemani, M., Valota, G., Bonfanti, A., Ciotti, A., Olofsson, U., Söderberg, A., Wahlström, J., Nosko, O., Straffelini, G., Gialanella, S., Ibrahim, M.: A concept for reducing PM10 emissions for car brakes by 50%. Wear **396-397**, 135–145 (2018). https://doi.org/https://doi.org/10.1016/j.wear.2017.06.018, http://www.sciencedirect.com/science/article/pii/S0043164817300960
15. Shin, H.: Replication Data for: Exposure to Traffic-related Air Pollution in Central Seoul using an Agent-based Framework (2021). https://doi.org/10.7910/DVN/C93XLZ, https://doi.org/10.7910/DVN/C93XLZ
16. Smit, R., Ntziachristos, L., Boulter, P.: Validation of road vehicle and traffic emission models - A review and meta-analysis. Atmospheric Environment **44**(25), 2943–2953 (2010). https://doi.org/10.1016/j.atmosenv.2010.05.022, http://dx.doi.org/10.1016/j.atmosenv.2010.05.022
17. TfL: Speed, Emissions, and Health (2018), http://content.tfl.gov.uk/speed-emissions-and-health.pdf
18. Tracy, M., Cerdá, M., Keyes, K.M.: Agent-Based Modeling in Public Health: Current Applications and Future Directions. Annual Review of Public Health **39**(1), 77–94 (apr 2018). https://doi.org/10.1146/annurev-publhealth-040617-014317, https://doi.org/10.1146/annurev-publhealth-040617-014317
19. Weinbruch, S., Worringen, A., Ebert, M., Scheuvens, D., Kandler, K., Pfeffer, U., Bruckmann, P.: A quantitative estimation of the exhaust, abrasion and resuspension components of particulate traffic emissions using electron microscopy. Atmospheric Environment **99**, 175–182 (2014). https://doi.org/10.1016/j.atmosenv.2014.09.075, http://dx.doi.org/10.1016/j.atmosenv.2014.09.075
20. Wilensky, U., Rand, W.: An introduction to agent-based modeling: modeling natural, social, and engineered complex systems with NetLogo. MIT Press (2015)
21. Zeng, W., Church, R.L.: Finding shortest paths on real road networks: the case for A*. International Journal of Geographical Information Science **23**(4), 531–543 (apr 2009). https://doi.org/10.1080/13658810801949850, https://doi.org/10.1080/13658810801949850